# Template Effects and Kinetic Selection in the Self-Assembly of Crown Ether Cyclobis(paraquat-*p*-phenylene) [2]Catenanes—Effect of the 1,4-Dioxybenzene and 1,5-Dioxynaphthalene Units

**Claudio D'Acerno,[a] Giancarlo Doddi,*[a] Gianfranco Ercolani,*[b] and Paolo Mencarelli*[a]**

**Abstract:** The template effects exerted by bis(*p*-phenylene)[34]crown-10 (**3**) and by 1,5-dinaphto[38]crown-10 (**4**) in the ring-closure reaction of the trication $\mathbf{2}^{3+}$ to yield the [2]catenanes $\mathbf{7}^{4+}$ and $\mathbf{8}^{4+}$ have been quantitatively evaluated in acetonitrile at 62 °C by UV/visible spectroscopy. The rate of ring closure of the trication $\mathbf{2}^{3+}$ dramatically increases in the presence of the templates **3** and **4**, up to approximately 230 times at $[\mathbf{3}] \approx 0.1\ \mathrm{mol\,L^{-1}}$, and up to approximately 1900 times at $[\mathbf{4}] \approx 0.01\ \mathrm{mol\,L^{-1}}$. The outcome of kinetic selection experiments, in which the two crown ethers compete for the incorporation into the catenane structure, has been discussed in the light of the obtained results. It has been shown that the product ratio of catenanes obeys the Curtin – Hammett principle only if the concentrations of the templates are equal and much greater than that of the substrate. Analysis of the rate profiles has shown that the 1,5-dioxynaphthalene unit, present in the template **4**, has a greater affinity than the 1,4-dioxybenzene unit, present in the template **3**, for the electron-deficient pyridinium rings present in both the transition-state and substrate structures. Ab initio calculations at the 3-21G and 6-31G(d) levels of theory indicate that the greater affinity of the 1,5-dioxynaphthalene unit cannot be explained on the basis of greater π – π stacking and [C–H ⋯ π] interactions, but rather on the basis of the model of apolar complexation in which the solvent plays a major role.

**Keywords:** ab initio calculations · catenanes · cyclizations · kinetics · supramolecular chemistry

## Introduction

In recent years there has been an increasing use of templates in synthesis which has enormously contributed to the development of supramolecular chemistry.[1] One of the most fruitful applications of templates is in the efficient preparation of interlocked rings, or catenanes, which until recently has eluded chemists.[2] The most common of the templated methods requires that one ring be thread by the precursor of the second ring, and the resulting assembly be held together as the second ring is formed. In other words, one macrocycle must act as a template for the formation of the second macrocycle.

Despite the numerous examples of template-directed syntheses of catenanes that can be found in the literature, no kinetic study of template effects in catenane formation has been reported to date, apart from a preliminary account of this work[3] and a competitive study aimed at obtaining the relative template abilities of two different crown ethers in the formation of [2]catenanes.[4]

In search of a suitable system for a kinetic investigation, we were attracted by the elegant reaction, shown in Scheme 1, which leads to the [2]catenane $\mathbf{7}^{4+}$. This was the first catenane synthesized by Stoddart and co-workers, in an extraordinary 70 % yield, from *p*-bis(bromomethyl)benzene and the dication $\mathbf{1}^{2+}$ in the presence of approximately three equivalents of bis(*p*-phenylene)[34]crown-10 (**3**) in acetonitrile.[5] Successively it was shown that 1,5-dinaphto[38]crown-10 (**4**) can be an even better template than the macrocyclic polyether **3**.[4] According to the mechanism proposed by Stoddart,[4, 6] one of the free nitrogen atoms of $\mathbf{1}^{2+}$ quaternizes upon treatment with the dihalide to afford the tricationic intermediate $\mathbf{2}^{3+}$. This can thread its way through the macrocyclic polyether's cavity of **3** or **4** to form the pseudorotaxane, or precatenane, $\mathbf{5}^{3+}$ or $\mathbf{6}^{3+}$, respectively, which are stabilized by a combination of π – π stacking, [C–H ⋯ O] hydrogen bonding, and [C–H ⋯ π] interactions.[7] The precatenane $\mathbf{5}^{3+}$ or $\mathbf{6}^{3+}$, is ideally predisposed to form the [2]catenane $\mathbf{7}^{4+}$ or $\mathbf{8}^{4+}$, respectively, by nucleophilic attack of the residual free nitrogen atom on the remaining benzylic halide site. The reaction therefore

---

[a] Prof. G. Doddi, Prof. P. Mencarelli, Dr. C. D'Acerno
Dipartimento di Chimica e Centro CNR
di Studio sui Meccanismi di Reazione
Università di Roma La Sapienza
P. le Aldo Moro 2, 00185 Roma (Italy)
Fax: (+39) 6-490631
E-mail: gdoddi@uniroma1.it, pmencarelli@uniroma1.it

[b] Prof. G. Ercolani
Dipartimento di Scienze e Tecnologie Chimiche
Università di Roma Tor Vergata
Via della Ricerca Scientifica, 00133 Roma (Italy)
Fax: (+39) 6-72594328
E-mail: ercolani@uniroma2.it

0947-6539/00/0619-3540 $ 17.50+.50/0

occurs in two steps, and only the second one would benefit from the template effect. This prompted us to carry out a detailed kinetic study in CH$_3$CN at 62 °C of the second step of the reaction shown in Scheme 1. The aim was to evaluate the template effects exerted by bis(*p*-phenylene)[34]crown-10 (**3**), and by 1,5-dinaphto[38]crown-10 (**4**) in the ring-closure reaction of the acyclic precursor $\mathbf{2}^{3+}$ to yield the [2]catenanes $\mathbf{7}^{4+}$ and $\mathbf{8}^{4+}$, respectively. The obtained results are the first quantitative data on template effects in the formation of catenanes. Moreover they allow a clearer discussion about the outcome of kinetic selection experiments in which two different crown ethers compete for incorporation into the catenane structure.

Ab initio calculations have been carried out in order to gain a deeper insight into the effects of the 1,4-dioxybenzene and 1,5-dioxynaphtalene units present in the macrocyclic templates.

## Results and Discussion

**Template effects and kinetic selection**: In a previous work we obtained, by $^1$H NMR in CD$_3$CN at 62 °C, the first-order rate constant ($k_0 = 8.3 \times 10^{-7}\,\mathrm{s}^{-1}$) for the cyclization of the trication $\mathbf{2}^{3+}$, in the absence of any added template, to yield cyclobis(paraquat-*p*-phenylene) ($\mathbf{9}^{4+}$) [Eq. (1)].[8]

In the present investigation we have studied the cyclization of the trication $\mathbf{2}^{3+}$ in the presence of the macrocyclic templates **3** and **4**, to yield the catenanes $\mathbf{7}^{4+}$ and $\mathbf{8}^{4+}$, respectively. The kinetics of the formation of catenanes $\mathbf{7}^{4+}$ and $\mathbf{8}^{4+}$ have been studied by UV/visible spectroscopy in acetonitrile at 62 °C. The appearance of their charge-transfer bands were observed at λ 470 nm and 529 nm, respectively. To avoid polymerization reactions, the concentration of the substrate $\mathbf{2}^{3+}$ was maintained as low as possible ($\approx 5-7 \times 10^{-4}\,\mathrm{mol\,L^{-1}}$). First-order rate constants ($k_{\mathrm{obs}}$) have been obtained in the presence of variable excess amounts of the polyether template **3** or **4**, up to their solubility limit ($\approx 0.1\,\mathrm{mol\,L^{-1}}$ and $\approx 0.01\,\mathrm{mol\,L^{-1}}$, respectively). The ratios

**Abstract in Italian:** *Gli effetti "template" esercitati dal bis-(p-fenilene)[34]corona-10 (**3**) e dall'1,5-dinafto[38]corona-[10] (**4**) nella reazione di chiusura d'anello del tricatione* $\mathbf{2}^{3+}$ *per dare i [2]catenani* $\mathbf{7}^{4+}$ *e* $\mathbf{8}^{4+}$ *sono stati determinati quantitativamente in acetonitrile a 62 °C tramite spettroscopia UV-Vis. La velocità di ciclizzazione del tricatione* $\mathbf{2}^{3+}$ *aumenta notevolmente in presenza degli eteri corona **3** e **4**, fino a circa 230 volte a [3] ≈ 0.1 mol L*$^{-1}$*, e fino a circa 1900 volte a [4] ≈ 0.01 mol L*$^{-1}$*. I risultati ottenuti permettono di discutere criticamente esperimenti cinetici competitivi nei quali i due eteri corona competono per essere incorporati nella struttura catenanica. In particolare si sottolinea che il rapporto dei catenani prodotti obbedisce il principio di Curtin–Hammett solo se la concentrazione dei "templates" è uguale tra loro, e molto più grande di quella del substrato. L'analisi dei profili di velocità ha mostrato che l'unità 1,5-diossinaftalenica, presente nell'etere corona **4**, ha un'affinità maggiore dell'unità 1,4-diossibenzenica, presente nell'etere corona **3**, nei confronti degli anelli piridinio, elettron-deficienti, presenti sia nella struttura dello stato di transizione che in quella del substrato. Calcoli ab-initio ai livelli di teoria 3–21G e 6–31G(d) indicano che la maggiore affinità dell'unità 1,5-diossinaftalenica non può essere spiegata sulla base di più forti interazioni [C–H ⋯ π] e di "stacking" π–π, ma piuttosto sulla base del modello della complessazione apolare nel quale il solvente gioca il ruolo principale.*

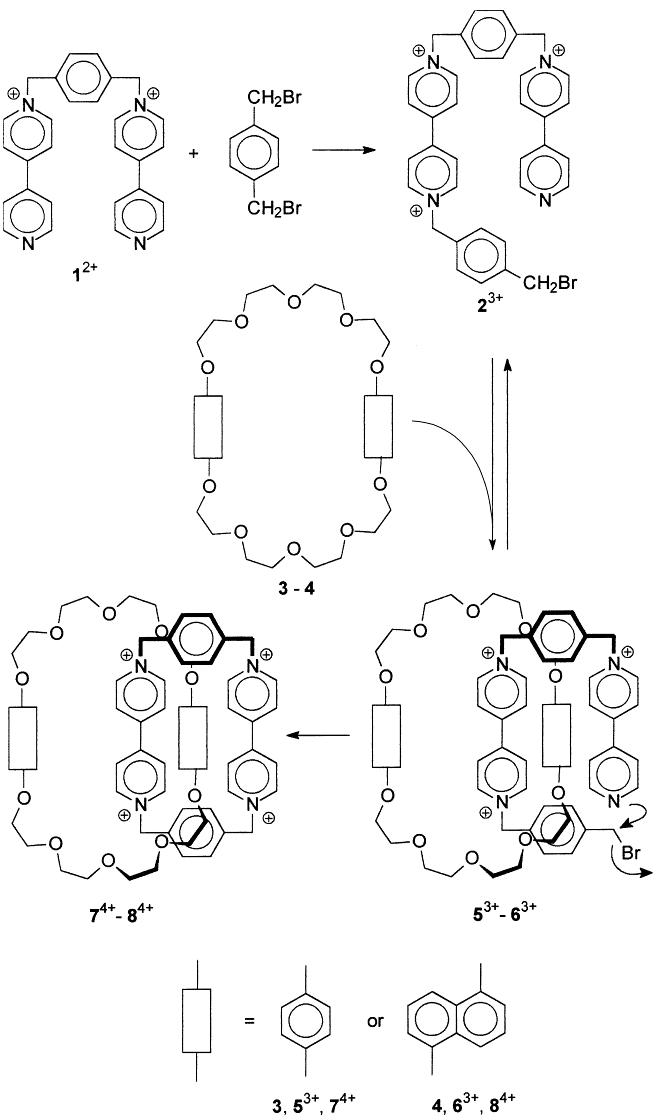

Scheme 1. Reaction scheme illustrating the formation of the catenanes $\mathbf{7}^{4+}$ and $\mathbf{8}^{4+}$.

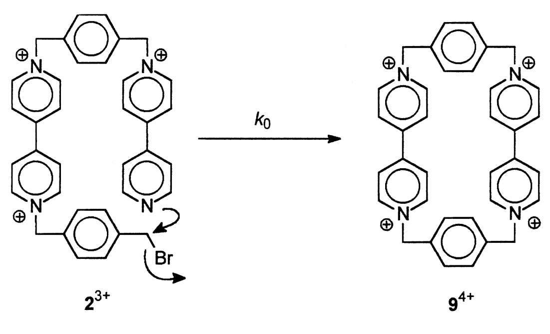

(1)

$k_{obs}/k_0$, plotted in Figures 1 and 2 against the concentration of **3** and **4**, respectively, provide a measure of the rate enhancements produced by the presence of the templates.

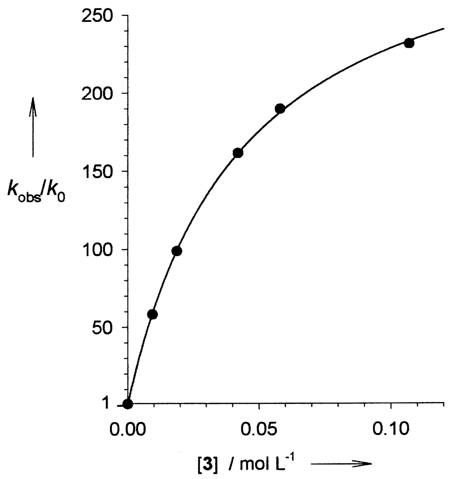

Figure 1. Rate enhancements produced by the macrocyclic template bis(*p*-phenylene)[34]crown-10 (**3**) on the ring closure of the trication $\mathbf{2}^{3+}$. The points are experimental and the curve is calculated (see text).

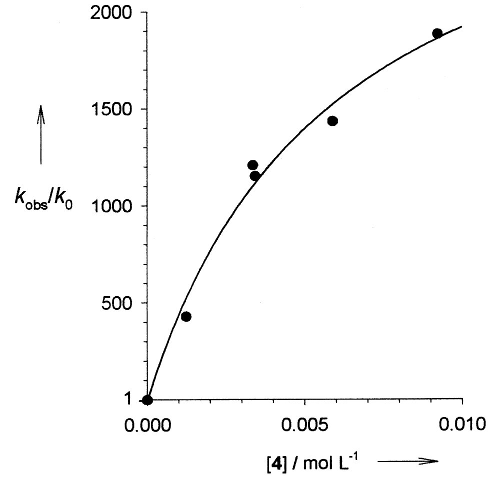

Figure 2. Rate enhancements produced by the macrocyclic template 1,5-dinaphto[38]crown-10 (**4**) on the ring closure of the trication $\mathbf{2}^{3+}$. The points are experimental and the curve is calculated (see text).

The data in Figure 1 shows that the ring closure of the trication $\mathbf{2}^{3+}$ is strongly accelerated by the presence of the template **3**, up to approximately 230 times at [**3**] ≈0.1 mol L$^{-1}$. This curve was the first to be obtained and the observed rate increase was considered to be of spectacular magnitude if compared with the known template effects produced by alkali and alkaline earth cations in the formation of crown ethers.[3] Now it is apparent (see Figure 2) that the template **4** is much more efficient: at a concentration of ≈0.01 mol L$^{-1}$, it produces a rate increase of almost 1900 times! This is by far the greatest template effect recorded up to now, and illustrates the fact that the magnitude of template effects is still largely unpredictable. To fully appreciate the significance of these rate increases, it is necessary to delve deep into the analysis of kinetic data.

On the basis of the mechanism suggested by Stoddart and co-workers,[4, 6] we propose that the operative kinetic scheme for the reaction is that depicted in Scheme 2, where the equilibrium for the formation of the precatenane is considered fast with respect to the ring-closure reactions. This is justified by the fact that the involved reactions of ring closure are very slow even at 62 °C. If the concentration of the template is in large excess with respect to that of the substrate, as in our experiments, its actual concentration can be assumed to be constant during the reaction course and coincident with its analytical concentration. Under this condition an apparent equilibrium constant $K = K_{sub}$[template] can be defined, so that the Winstein–Holness equation[9] can be applied to Scheme 2. Accordingly Equation (2) holds, in which $c_{sub}$ is the total concentration of the substrate $\mathbf{2}^{3+}$, irrespective of the various forms actually present in solution through the establishment of mobile equilibria (in the present case, $c_{sub}$ is the sum of the concentrations of free $\mathbf{2}^{3+}$ and of the precatenane $\mathbf{5}^{3+}$ or $\mathbf{6}^{3+}$), and $k_{obs}$ is the observed first-order rate constant given by the Winstein–Holness expression [Eq. (3)]. The rate increase produced by the template, $k_{obs}/k_0$, is then given, if one takes the definition of $K$ into consideration, by Equation (4).

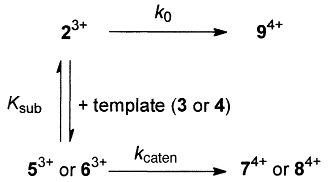

Scheme 2. Kinetic scheme for the reaction of the trication $\mathbf{2}^{3+}$ in the presence of the template **3** or **4**.

$$-\frac{dc_{sub}}{dt} = k_{obs}c_{sub} \tag{2}$$

$$k_{obs} = \frac{k_0 + k_{caten}K}{1 + K} \tag{3}$$

$$\frac{k_{obs}}{k_0} = \frac{1 + \frac{k_{caten}K_{sub}}{k_0}[\text{template}]}{1 + K_{sub}[\text{template}]} \tag{4}$$

Since the principal tenet of transition-state theory is the assumption of an equilibrium between reactants and transition state, it could be easily shown that the term $k_{caten}K_{sub}/k_0$ is the association constant ($K_{T\#}$) of the template with the cyclic transition state as illustrated in Equation (5). Accordingly Equation (4) reduces to Equation (6), showing that a rate enhancement will be observed if the template binds the transition state more strongly than the reactants.[10, 11]

$$\frac{k_{obs}}{k_0} = \frac{1 + K_{T\#}[\text{template}]}{1 + K_{sub}[\text{template}]} \tag{6}$$

Non-linear least-squares treatment of the $k_{obs}/k_0$ ratios according to Equation (6) afforded the $K_{sub}$ and $K_{T\#}$ values listed in Table 1. How closely Equation (6) fits the data is shown by the curves drawn in Figures 1 and 2. Both curves show a clear tendency to saturation. The saturation value, which is given by the ratio $k_{caten}/k_0 = K_{T\#}/K_{sub}$, also reported in Table 1, is the maximum theoretical rate enhancement that

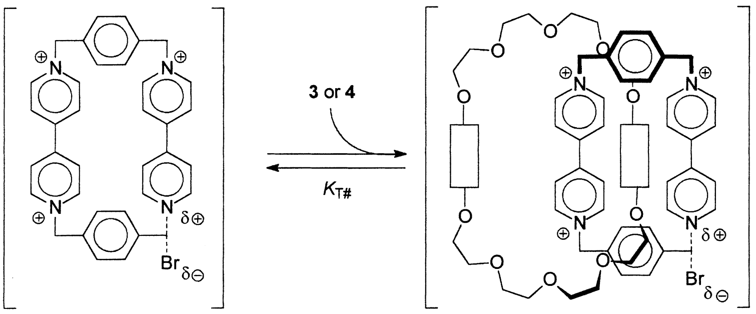

(5)

Table 1. Kinetic and thermodynamic constants in $CH_3CN$ at 62 °C.

| Template | $K_{sub}$ [L mol$^{-1}$] | $K_{T\#}$ [L mol$^{-1}$] | $K_{T\#}/K_{sub}$ | $k_{caten}$ [s$^{-1}$] |
|---|---|---|---|---|
| **3** | $23 \pm 1$ | $(7.5 \pm 0.2) \times 10^3$ | $328 \pm 5$ | $(2.72 \pm 0.04) \times 10^{-4}$ |
| **4** | $170 \pm 40$ | $(5.1 \pm 0.7) \times 10^5$ | $(3.1 \pm 0.4) \times 10^3$ | $(2.6 \pm 0.3) \times 10^{-3}$ |

would be attained when the substrate is completely bound to the template. These values indicate that the precatenanes $\mathbf{5}^{3+}$ and $\mathbf{6}^{3+}$ are 328 and 3100 times, respectively, more reactive than the free ligand $\mathbf{2}^{3+}$. Such spectacular rate enhancements are due to the fact that the associations of the acyclic trication $\mathbf{2}^{3+}$ with the templates **3** and **4** are rather weak, whereas the cyclic transition state shows a much greater ligand affinity towards them. This is mainly due to the preorganization of the cyclic transition state and, secondarily, to the development of a further positive charge on the initially neutral nitrogen atom.

In a previous work we studied the template effect exerted by $p\text{-}C_6H_4(OCH_2CH_2OCH_2CH_2OH)_2$ (**10**) on the reaction reported in Equation (1) and obtained the following values for the association constants: $K_{T\#} = 144\ \mathrm{L\,mol^{-1}}$ and $K_{sub} = 1.9\ \mathrm{L\,mol^{-1}}$.[8] The greater associations shown by the cyclic template **3** with respect to the acyclic template **10** can be mainly attributed to the operation of two factors. These are: i) the greater π surface of template **3** which should provide stronger stabilizing interactions with the pyridinium rings of both the substrate and the transition state, and ii) the preorganization of the cyclic template which is lacking in the acyclic one. It was suggested that the oxygen atoms of the polyether chains significantly contribute to the binding by [C–H ··· O] hydrogen bonds with the α-protons of the pyridinium rings.[7] These interactions, which involve a reduction of the rotational entropy of the polyethereal chains, should be more favorable with the preorganized cyclic template **3**.

Before comparing the effects of the 1,4-dioxybenzene and 1,5-dioxynaphthalene units present in the structure of the templates **3** and **4**, respectively, it is useful to consider the expected outcome of a kinetic selection experiment, particularly in light of the results reported in Table 1. Let us consider a competitive reaction in which the substrate $\mathbf{2}^{3+}$ reacts in the presence of both the templates **3** and **4** as shown in Scheme 3. The rate of formation of the two catenanes is given by Equations (7) and (8).

$$\frac{d[\mathbf{7}^{4+}]}{dt} = k_{caten(3)}[\mathbf{5}^{3+}] \tag{7}$$

$$\frac{d[\mathbf{8}^{4+}]}{dt} = k_{caten(4)}[\mathbf{6}^{3+}] \tag{8}$$

Considering the ratio of Equation (8) to Equation (7) and the definition of the association constants $K_{sub(3)}$ and $K_{sub(4)}$ illustrated in Scheme 3, Equation (9) is easily obtained.

$$\frac{d[\mathbf{8}^{4+}]}{d[\mathbf{7}^{4+}]} = \frac{k_{caten(4)} K_{sub(4)} [\mathbf{4}]}{k_{caten(3)} K_{sub(3)} [\mathbf{3}]} \tag{9}$$

If the concentrations of the templates **3** and **4** are in large excess with respect to the concentration of the substrate, their actual concentrations can be assumed to be constant during the reaction course and coincident with their analytical concentrations. Since, with the assumption made, the right-hand side of Equation (9) is constant, one can easily integrate to obtain Equation (10),

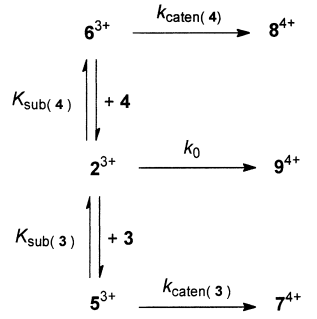

Scheme 3. Kinetic scheme for the competitive reaction of the trication $\mathbf{2}^{3+}$ in the presence of the templates **3** and **4**.

$$\frac{[\mathbf{8}^{4+}]}{[\mathbf{7}^{4+}]} = \frac{k_{caten(4)} K_{sub(4)} [\mathbf{4}]}{k_{caten(3)} K_{sub(3)} [\mathbf{3}]} \tag{10}$$

which gives the ratio of the formed catenanes at the completion of reaction (or at any intermediate point). In other words, the condition that the concentration of the templates is much greater than that of the substrate makes the Curtin–Hammett principle[9] applicable to Scheme 3. In fact, considering that $k_{caten(4)}K_{sub(4)}/k_0 = K_{T\#(4)}$ and $k_{caten(3)}K_{sub(3)}/k_0 = K_{T\#(3)}$, Equation (10) can be rewritten in the form of Equation (11) which illustrates the fact that if the

$$\frac{[\mathbf{8}^{4+}]}{[\mathbf{7}^{4+}]} = \frac{K_{T\#(4)} [\mathbf{4}]}{K_{T\#(3)} [\mathbf{3}]} \tag{11}$$

concentrations of the templates, besides being in large excess are also equal, the relative amounts of the produced catenanes depend only on the relative stabilization of the transition state brought about by the templates **4** and **3**. A subtle point becomes relevant here: although the ratio $K_{T\#(4)}/K_{T\#(3)}$ is a measure of the relative ability of the two templates to be trapped in the catenane structure in competitive experiments, it cannot be considered a measure of their relative template effect. In fact, as illustrated by Figures 1 and 2, and by Equation (6), the template effect is dependent on the template concentration up to saturation, and when saturation is reached, the relative template effect would be given by $(K_{T\#(4)}/K_{T\#(3)})/(K_{sub(4)}/K_{sub(3)}) = k_{caten(4)}/k_{caten(3)}$. In other words, one cannot be sure that the macrocyclic template which is most easily incorporated into the catenane structure will also be that which produces the highest rate enhancement. To estimate the relative template effect, the data from competitive experiments should be corrected by the relative binding of the substrate towards the two templates.

From the $K_{T\#}$ data in Table 1, the product ratio of the catenanes $\mathbf{8}^{4+}$ and $\mathbf{7}^{4+}$ formed in the presence of a large excess of equimolar amounts of the templates **3** and **4** should be $68 \pm 11$. If the templates are not in large excess with respect to the substrate, their actual concentrations are time dependent and Equation (9) cannot be immediately integrated. The consequences are that, under these experimental conditions, the Curtin–Hammett principle is not valid, and the product ratio depends not only on time (and percentage reaction) but also on the chosen initial concentrations. To investigate the effect of substrate and template concentrations on the final ratio of the catenanes, we have carried out several numerical integrations of the rate equations pertinent to Scheme 3 with the kinetic and thermodynamic constants reported in Table 1. The obtained results are plotted in Figure 3 as a family of curves which represent constant ratios of the initial concentration of substrate to that of the templates, with the templates always present in equimolar amounts. From Figure 3 it appears that the maximum selectivity corresponds to the Curtin–Hammett limit that is reached when the templates are in large excess with respect to the substrate (the lower the template/substrate ratio the lower the selectivity). The lower selectivity is caused by a progressive imbalance of the actual concentration of the two templates during the reaction: the more easily formed catenane causes a greater reduction of the concentration of the corresponding template and thus slows down its own formation. In other words, there is a sort of negative feedback that is the origin of the leveling effect on selectivity. It is interesting to note that the selectivity tends to increase with increasing dilution up to the Curtin–Hammett limit.[12] The explanation for this phenomenon is best illustrated by the curve in Figure 3 which refers to the ratio $[\mathbf{2}^{3+}]_0:[\mathbf{4}]_0:[\mathbf{3}]_0 = 1:0.5:0.5$. It is evident that if the catenanes were the only products of the reaction under this condition, there would not be any competition between the two templates since the amount of substrate would be sufficient to incorporate both of them. In fact a lack of selectivity is observed, but only in concentrated solutions. At low substrate (and template) concentration another reaction becomes important, namely the unassisted ring closure of the substrate [Eq. (1)], which being a true first-order reaction has a rate that decreases less on dilution than the catenation processes. At high dilution, when it is the principal process, only a small fraction of the substrate undergoes catenation; this small fraction is not sufficient to cause an imbalance in the concentrations of the templates, so the Curtin–Hammett limit can still be reached at very high dilution. Apart from this curious phenomenon, the conclusion is that if a large excess of templates is not used in competitive experiments, the observed selectivity can be much lower than the maximum one (the Curtin–Hammett limit) and depends on a complex interplay of kinetic and thermodynamic constants.

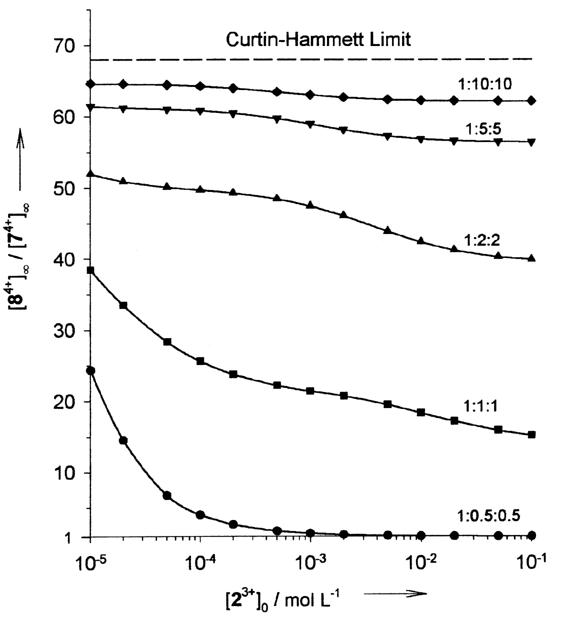

Figure 3. Calculated values of the product ratio of the catenanes in the competitive reaction shown in Scheme 3 as a function of initial concentration of substrate. Each curve refers to a constant ratio of the initial concentration of substrate to that of the templates ($[\mathbf{2}^{3+}]_0:[\mathbf{4}]_0:[\mathbf{3}]_0$) indicated next to the curve.

**1,4-Dioxybenzene unit versus 1,5-dioxynaphthalene unit**: From a comparison of the data in Table 1, it appears that the greater template effect shown by the template **4** is the result of a greater selectivity of the preorganized cyclic transition state ($K_{T\#(4)}/K_{T\#(3)} \approx 70$) with respect to that of the linear substrate ($K_{sub(4)}/K_{sub(3)} \approx 7$). However, both these values indicate that the 1,5-dioxynaphthalene unit has a greater affinity than the 1,4-dioxybenzene unit for the electron-deficient pyridinium rings present in the transition-state and substrate structures. Various binding data in the literature that relate to the host cyclobis(paraquat-*p*-phenylene) ($\mathbf{9}^{4+}$) in MeCN at 298 °C,[13, 14] support this conclusion, for example, 1,5-naphthalenediol ($K = 7.7 \times 10^2$ L mol$^{-1}$) versus hydroquinone ($K = 18$ L mol$^{-1}$) and 1,5-bis[2-(2-hydroxyethoxy)ethoxy]naphthalene ($K = 2.5 \times 10^4$ L mol$^{-1}$) versus 1,4-bis[2-(2-hydroxyethoxy)ethoxy]benzene (**10**) ($K = 3.4 \times 10^3$ L mol$^{-1}$). To gain a deeper insight into the factors that cause the 1,5-dioxynaphtalene core to be more effective than the 1,4-dioxybenzene one, we undertook an ab initio computational study.

Earlier computational studies of inclusion complexes of aromatic guests with the tetracation $\mathbf{9}^{4+}$ were based on molecular mechanics,[15, 16] Monte Carlo method with an empirical force field,[16] AM1 and PM3 semiempirical methods.[14, 17–20] Rather surprisingly only few ab initio calculations, at the RHF/STO-3G level of theory, have been reported.[19]

Our aim was to evaluate the gas-phase binding energy of the host cyclobis(paraquat-*p*-phenylene) ($\mathbf{9}^{4+}$) with the guests 1,4-dimethoxybenzene (**11**) and 1,5-dimethoxynaphthalene (**12**) by ab initio calculations. Host–guest complexation in the gas phase is essentially a single-step event ($H + G \rightleftarrows HG$), to which an energy change corresponding to the complexation energy, $\Delta E_C$ is associated. This can be easily evaluated from the ab initio energies of the host, of the guest, and of the host–guest complex ($\Delta E_C = E_{HG} - E_H - E_G$). However, it is well known that the use of a limited basis set introduces the so-called basis set superposition error (BSSE) that can be approximately accounted for by the counterpoise correction, $\Delta E_{CP}$ (see Experimental Section for details).[21] The counterpoise corrected complexation energy is then given by $\Delta E_C - \Delta E_{CP}$.

We have carried out full geometry optimizations, with the RHF/3-21G basis set, of all the species involved in the calculation of $\Delta E_C$, for both the guests **11** and **12**. The starting structures of the host–guest complexes were approximately centrosymmetrical as suggested by the X-ray structures of the catenanes **7**$^{4+}$ and **8**$^{4+}$, which show an aromatic core located at the center of the cavity of cyclobis(paraquat-*p*-phenylene).[5a, 22] The final optimized structures have almost $C_i$ symmetry. The lowest energy conformation of the tetracation **9**$^{4+}$ has almost $C_{2h}$ symmetry (the $C_2$ axis passes through the 4-4′ bond of the two paraquat units). On the basis of a conformational search using the PM3 semiempirical method, Evanseck et al. concluded that the $D_2$ structure of **9**$^{4+}$ is the most stable,[19] and accordingly carried out 3-21G and 6-31G(d) calculations of **9**$^{4+}$ by imposing this symmetry constraint (see Supplementary Material of ref. [19]). In contrast, our findings indicate that, at the 3-21G and 6-31G(d) levels of theory, the $C_{2h}$ structure is 4.7 and 3.0 kcal mol$^{-1}$, respectively, lower in energy than the $D_2$ structure. For the guests **11** and **12**, the most stable conformations have a transoid structure (in the case of **12**, with the methyl groups pointing away from the hydrogens in peri position) of almost $C_{2h}$ symmetry.

We also carried out calculations with the RHF/6-31G(d) basis set. However, to speed up the calculations with this more extended basis set, we imposed the center of symmetry as a constraint for the geometry optimization of all the involved species. This appeared justified to us, since the calculations with the 3-21G basis set showed this element of symmetry to be common to all the species. Uncorrected and counterpoise corrected binding energies, computed from RHF/3-21G and RHF/6-31G(d) levels of theory, are reported in Table 2. The data show the importance of counterpoise correction, which largely dominates the values of $\Delta E_C$, especially, as expected, in the case of the less extended basis set, namely 3-21G. The most striking result is that corrected complexation energies are relatively small for gas phase host–guest complexations, and show a trend that is the opposite of that observed in solution, that is, in the gas phase the 1,4-dioxybenzene unit shows a greater affinity for the host **9**$^{4+}$ than the 1,5-dioxynaphthalene unit, and moreover, the interaction between the latter unit and the host **9**$^{4+}$ appears to be unfavorable. The two basis sets give consistent results; in both cases the guest **11** is more strongly complexed than the guest **12** by approximately 5–6 kcal mol$^{-1}$, and in both cases the corrected complexation energy of guest **11** is negative, whereas that of guest **12** is positive. Overall these results indicate that π–π stacking and [C–H···π] interactions between the electron-deficient cyclobis[paraquat-*p*-phenylene] and electron-rich aromatic guests cannot be held responsible for the observed associations in solutions, and rather suggest that solvent interactions play the major role. In our opinion, the strength of complexation between the host **9**$^{4+}$ and aromatic guests in solution can be most easily explained on the basis of the model of apolar complexation. This model has been discussed at length by Diederich,[23a] and by Diederich and Smithrud,[23b] who pointed out the importance of solvent cohesive interactions and polarizability as the major factors that control apolar binding strength. According to this model, which has general validity, solvent molecules solvate apolar solutes by forming an ordered cluster around the apolar surface. When the solute is complexed by a host, besides the evident gain of host–guest interactions and loss of solvent–guest interactions, there is a gain of solvent cohesive interactions and entropy, due to the collapse of the ordered solvent cluster into the bulk. This gain would be greater for the naphthalenic core with respect to the benzenic core because of the greater apolar surface of the former. Apolar binding is generally strongest in solvents with low molecular polarizability and with high cohesive interactions, and it has been suggested that the empirical solvent polarity parameters $E_T(30)$ for the various solvents represent a good measure of the interplay between these two factors.[22] That the driving force for the complexation of aromatic guests by the tetracation **9**$^{4+}$ is apolar binding would be also confirmed by a study of solvent effects on the binding equilibria between **9**$^{4+}$ and the guests indole and catechol.[24] The authors reported good linear free-energy relationships between the free energies of complexation and the polarity of the solvent, as measured by *Z*-values or $E_T(30)$ values, indicative of apolar binding complexation.

In conclusion, two structural features are required for optimum complexation of a guest molecule by cyclobis[paraquat-*p*-phenylene], namely an aromatic core, which is essential in placing the guest in the host cavity by the mechanism of apolar complexation, and two side arms with suitably placed oxygen atoms that interact with the acidic α-hydrogens of the pyridinium rings of the host by [C–H···O] hydrogen bonding. While the importance of the latter interaction has been adequately emphasized in the literature,[7] we wish to draw attention to the importance of the apolar complexation of the aromatic core.

Table 2. Computed uncorrected and counterpoise corrected complexation energies in kcal mol$^{-1}$, using RHF/3–21G and RHF/6-31G* levels of theory.

| Guest | $\Delta E_C$ (3–21G) | $\Delta E_C - \Delta E_{CP}$ (3-21G) | $\Delta E_C$ (6-31G*) | $\Delta E_C - \Delta E_{CP}$ (6-31G*) |
|---|---|---|---|---|
| **11** | −14.9 | −1.1 | −9.0 | −3.1 |
| **12** | −14.2 | +3.9 | −6.4 | +2.7 |

## Experimental Section

**Materials and methods**: 1,1″-[1,4-Phenylenebis(methylene)]-1′-[4-(bromomethyl)benzyl]bis(4,4′-bipyridinium) tris(hexafluorophosphate) (**2**$^{3+}$·3PF$_6$) was from our previous work.[8] HPLC grade acetonitrile (Carlo Erba) was used in the kinetic experiments without further purification. UV/Vis spectra and kinetic measurements were carried out on a Perkin–Elmer Lambda18 spectrophotometer. Numerical integrations of differential rate equations were performed by using the program Scientist for Windows, Version 2.0 from Micromath, Salt Lake City, Utah. Ab initio calculations were performed with the GAUSSIAN 98 software package.[25]

**Kinetic measurements**: Kinetic measurements were carried out, at 62 °C in acetonitrile, in a 3 mL cuvette (optical path 1 cm) kept in the thermostatted cell compartment of the spectrophotometer. In a typical run, a solution (0.0193 mol L$^{-1}$) of $\mathbf{2}^{3+}\cdot 3\,PF_6$ (100 µL) was added to a solution of either the template **3** or **4** (2.5 mL) at the appropriate concentration (see below).The appearance of the charge-transfer band of the catenane $\mathbf{7}^{4+}$ or $\mathbf{8}^{4+}$ was followed at λ470 or 529 nm, respectively. In all cases, first-order behavior was observed. Relative kinetic constants ($k_{obs}/k_0$, where $k_0 = 8.3\times10^{-7}\,s^{-1}$) at the various template concentrations (corrected for the volume increase at 62 °C and given in parentheses in mol L$^{-1}$ were as follows: Template **3**: 1 (0), 58.4 ($9.50\times10^{-3}$), 99.0 ($1.88\times10^{-2}$), 161.8 ($4.20\times10^{-2}$), 190.2 ($5.80\times10^{-2}$), 232.0 ($1.07\times10^{-1}$). Data plotted in Figure 1. Template **4**: 1 (0), 430 ($1.24\times10^{-3}$), 1210 ($3.36\times10^{-3}$), 1154 ($3.43\times10^{-3}$), 1436 ($5.90\times10^{-3}$), 1886 ($9.24\times10^{-3}$). Data plotted in Figure 2.

**Numerical integrations**: Numerical integrations of the differential rate equations pertinent to Scheme 3 were carried out by the program Scientist for Windows. In the formulation of the rate equations, the equilibria in the scheme were considered as the result of a forward kinetic constant and a reverse kinetic constant; for example, we considered $K_{sub(\mathbf{3})} = k_{sub(\mathbf{3})f}/k_{sub(\mathbf{3})r}$. In all of the cases an arbitrary, yet very high, value was attributed to the reverse kinetic constant, that is, $1\times10^{6}\,s^{-1}$, so that the forward kinetic constant was calculated by the known equilibrium constant; for example, $k_{sub(\mathbf{3})f} = 1\times10^{6}\,K_{sub(\mathbf{3})}$. Such high values, if compared with the values of the other kinetic constants involved in Scheme 3, guarantee the attainment of the corresponding equilibrium during the reaction course.

**Counterpoise correction**: The evaluation of counterpoise correction, $\Delta E_{CP}$, was carried out according to the following equation:[21] $\Delta E_{CP} = E^{*}_{H(hg)} + E^{*}_{G(hg)} - E^{*}_{H(h)} - E^{*}_{G(g)}$, where the asterisk denotes single-point calculations carried out at the geometry that each fragment has in the host–guest complex. In parentheses the used basis set is indicated. For example, $E^{*}_{H(hg)}$ indicates a single point energy calculation of the host, H, carried out with the geometry it has in the complex, in the presence of the normal h basis functions and with the g basis functions of guest G as ghost orbitals.

---

[1] For general reviews on template effects, see: a) S. Anderson, H. Anderson, J. K. Sanders, *Acc. Chem. Res.* **1993**, *26*, 469–475; b) R. Hoss, F. Vögtle, *Angew. Chem.* **1994**, *106*, 389; *Angew. Chem. Int. Ed. Engl.* **1994**, *33*, 375–384; c) D. H. Busch, A. L. Vance, A. G. Kolchinski in *Comprehensive Supramolecular Chemistry, Vol. 9* (Eds.: J. L. Atwood, J. E. D. Davies, D. D. MacNicol, F. Vögtle, J.-P Sauvage, M. W. Hosseini), Pergamon, Oxford, **1996**, Chapter 1; d) N. V. Gerbeleu, V. B. Arion, J. Burgess, *Template Synthesis of Macrocyclic Compounds*, Wiley-VCH, **1999**; e) *Templated Organic Synthesis* (Eds.: F. Diederich, P. J. Stang), Wiley-VCH, **2000**.

[2] For reviews on template-directed syntheses of catenanes, see:a) C. O. Dietrich-Buchecker, J.-P. Sauvage, *Chem. Rev.* **1987**, *87*, 795–810; b) C. O. Dietrich-Buchecker, J.-P. Sauvage, *Bioorg. Chem. Front.* **1991**, *2*, 195–248; c) D. B. Amabilino, J. F. Stoddart, *Chem. Rev.* **1995**, *95*, 2725–2828; d) D. Philp, J. F. Stoddart, *Angew. Chem.* **1996**, *108*, 1242–1286; *Angew. Chem. Int. Ed. Engl.* **1996**, *35*, 1154–1196; e) J.-C. Chambron, C. O. Dietrich-Buchecker, J.-P. Sauvage in *Comprehensive Supramolecular Chemistry, Vol. 9* (Eds.: J. L. Atwood, J. E. D. Davies, D. D. MacNicol, F. Vögtle, J.-P Sauvage, M. W. Hosseini), Pergamon, Oxford, **1996**, Chapter 2; f) F. M. Raymo, J. F. Stoddart in *Comprehensive Supramolecular Chemistry, Vol. 9* (Eds.: J. L. Atwood, J. E. D. Davies, D. D. MacNicol, F. Vögtle, J.-P Sauvage, M. W. Hosseini), Pergamon, Oxford, **1996**, Chapter 3; g) M. Fujita in *Comprehensive Supramolecular Chemistry, Vol. 9* (Eds.: J. L. Atwood, J. E. D. Davies, D. D. MacNicol, F. Vögtle, J.-P Sauvage, M. W. Hosseini), Pergamon, Oxford, **1996**, Chapter 7; h) M. Belohradsky, F. M. Raymo, J. F. Stoddart, *Collect. Czech. Chem. Commun.* **1997**, *62*, 527–557; i) *Molecular Catenanes, Rotaxanes and Knots* (Eds.: J.-P. Sauvage, C. O. Dietrich-Buchecker), Wiley-VCH, **1999**.

[3] S. Capobianchi, G. Doddi, G. Ercolani, P. Mencarelli, *J. Org. Chem.* **1998**, *63*, 8088–8089.

[4] D. B. Amabilino, P. R. Ashton, L. Perez-Garcìa, J. F. Stoddart, *Angew. Chem.* **1995**, *107*, 2569–2572; *Angew. Chem. Int. Ed. Engl.* **1995**, *34*, 2378–2380.

[5] a) P. R. Ashton, T. T. Goodnow, A. E. Kaifer, M. V. Reddington, A. M. Z. Slawin, N. Spencer, J. F. Stoddart, C. Vicent, D. J. Williams, *Angew. Chem.* **1989**, *101*, 1404–1408; *Angew. Chem. Int. Ed. Engl.* **1989**, *28*, 1396–1399; b) P. L. Anelli, P. R. Ashton, R. Ballardini, V. Balzani, M. Delgado, M. T. Gandolfi, T. T. Goodnow, A. E. Kaifer, D. Philp, M. Pietraszkiewicz, L. Prodi, M. V. Reddington, A. M. Z. Slawin, N. Spencer, J. F. Stoddart, C. Vicent, D. J.Williams, *J. Am. Chem. Soc.* **1992**, *114*, 193–218.

[6] C. L. Brown, D. Philp, N. Spencer, J. F. Stoddart, *Isr. J. Chem.* **1992**, *32*, 61–67.

[7] K. N. Houk, S. Menzer, S. P. Newton, F. M. Raymo, J. F. Stoddart, D. J. Williams, *J. Am. Chem. Soc.* **1999**, *121*, 1479–1487, and references cited therein.

[8] S. Capobianchi, G. Doddi, G. Ercolani, J. W. Keyes, P. Mencarelli, *J. Org. Chem*, **1997**. *62*, 7015–7017.

[9] E. L. Eliel, S. H. Wilen, *Stereochemistry of Carbon Compounds*, Wiley, New York, **1994**, pp. 647–655.

[10] R. Cacciapaglia, L. Mandolini, *Chem. Soc. Rev.* **1993**, *22*, 221–231.

[11] J. Kraut, *Science* **1988**, *242*, 533–540.

[12] Although this is not evident from Figure 3, it has been verified by performing numerical integration at substrate concentrations lower than those reported in Figure 3.

[13] M. Asakawa, W. Dehaen, G. L'abbé, S. Menzer, J. Nouwen, F. M. Raymo, J. F. Stoddart, D. J. Williams, *J. Org. Chem.* **1996**, *61*, 9591–9595.

[14] R. Castro, K. R. Nixon, J. D. Evanseck, A. E. Kaifer, *J. Org. Chem.* **1996**, *61*, 7298–7303.

[15] H. G. Ricketts, J. F. Stoddart, M. M. Hann in *Computational Approaches in Supramolecular Chemistry* (Ed.: G. Wipff), Kluwer Academic, Boston, MA, **1994**.

[16] G. A. Kaminski, W. L. Jorgensen, *J. Chem. Soc. Perkin Trans. 2* **1999**, 2365–2375.

[17] E. A. Smit, R. R. Lilienthal, R. J. Fonseca, D. K. Smit, *Anal. Chem.* **1994**, *66*, 3013–3020.

[18] B. Odell, M. V. Reddington, A. M. Z. Slawin, N. Spencer, J. F. Stoddart, D. J. Williams, *Angew. Chem.* **1988**, *101*, 1605; *Angew. Chem. Int. Ed. Engl.* **1988**, *27*, 1547–1550.

[19] R. Castro, M. J. Berardi, E. Córdova, M. Ochoa de Olza, A. E. Kaifer, J. D. Evanseck, *J. Am. Chem. Soc.* **1996**, *118*, 10257–10268.

[20] R. Castro, P. D. Davidov, K. A. Kumar, A. P. Marchand, J. D. Evanseck, A. E. Kaifer, *J. Phys. Org. Chem.* **1997**, *10*, 369–382.

[21] F. Jensen, *Introduction to Computational Chemistry*, Wiley, Chichester, **1999**, pp. 172–173.

[22] P. R. Ashton, C. L. Brown, E. J. T. Chrystal, T. T. Goodnow, A. E. Kaifer, K. P. Parry, D. Philp, A. M. Z. Slawin, N. Spencer, J. F. Stoddart, D. J. Williams, *J. Chem. Soc. Chem. Commun.* **1991**, 634–639.

[23] a) F. Diederich, *Cyclophanes (Monographs in Supramolecular Chemistry)* (Ed.: J. F. Stoddart), RSC, Cambridge, UK, **1991**, Chapter 7; b) D. B. Smithrud, F. Diederich, *J. Am. Chem. Soc.* **1990**, *112*, 339–343.

[24] A. Mirzoian, A. E. Kaifer, *J. Org. Chem.* **1995**, *60*, 8093–8095.

[25] M. J. Frisch, G. W. Trucks, H. B. Schlegel, G. E. Scuseria, M. A. Robb, J. R. Cheeseman, V. G. Zakrzewski, J. A. Montgomery, Jr., R. E. Stratmann, J. C. Burant, S. Dapprich, J. M. Millam, A. D. Daniels, K. N. Kudin, M. C. Strain, O. Farkas, J. Tomasi, V. Barone, M. Cossi, R. Cammi, B. Mennucci, C. Pomelli, C. Adamo, S. Clifford, J. Ochterski, G. A. Petersson, P. Y. Ayala, Q. Cui, K. Morokuma, D. K. Malick, A. D. Rabuck, K. Raghavachari, J. B. Foresman, J. Cioslowski, J. V. Ortiz, A. G. Baboul, B. B. Stefanov, G. Liu, A. Liashenko, P. Piskorz, I. Komaromi, R. Gomperts, R. L. Martin, D. J. Fox, T. Keith, M. A. Al-Laham, C. Y. Peng, A. Nanayakkara, C. Gonzalez, M. Challacombe, P. M. W. Gill, B. Johnson, W. Chen, M. W. Wong, J. L. Andres, C. Gonzalez, M. Head-Gordon, E. S. Replogle, J. A. Pople, *Gaussian 98,* Revision A.7, Gaussian, Pittsburgh PA, **1998**.

Received: December 27, 1999 [F2211]